2026-11-02
The self-archived post print version of this conference paper is available at Linköping University Institutional Repository (DiVA):
https://urn.kb.se/resolve?urn=urn:nbn:se:liu:diva-229008

Experimental Validation of Wary Control with Stationary Obstacle

Victor Fors, Björn Olofsson, Lars Nielsen and J. Christian Gerdes

In: Proceedings of 17th International Symposium on Advanced Vehicle Control (AVEC'26) 7-11 September 2026, 2026,
Publisher: Society of Automotive Engineers of Japan, Inc.

N.B.: When citing this work, cite the original publication.

Copyright holder: See original publication

LINKÖPING UNIVERSITY

Proceedings of 17th International Symposium on Advanced Vehicle Control (AVEC'26)
7-11 September 2026, Tsukuba, Japan
Wed-PM1-C-5
20269477

Experimental Validation of Wary Control with Stationary Obstacle

Victor Fors [1], Björn Olofsson [2,3], Lars Nielsen [3], J. Christian Gerdes [1]

1) Department of Mechanical Engineering, Stanford University, USA
2) Department of Automatic Control, Lund University, Sweden
3) Department of Electrical Engineering, Linköping University, Sweden
(Corresponding author: lars.nielsen@liu.se)

Abstract: Wary control for emergency avoidance is demonstrated to perform well in real vehicle experiments. For emergency braking, it is well known that anti-lock braking is very successful. That control algorithm does not use, nor know, the actual friction. However, the outcome, the result, depends on actual friction since the stopping distance is longer for low friction. In the same spirit, wary control is an algorithm for emergency avoidance that does not know nor use any knowledge about the actual friction coefficient. As for braking, the result, how quickly an obstacle can be cleared, depends on actual friction. Wary control has been implemented in the Stanford X1 vehicle, and it has been tested and evaluated by experiments at the Thunderhill Raceway Park.

Keywords: Vehicle Feedback Control, Automated Driving, Safety-Critical Handling, Emergency Avoidance, At-the-Limit Maneuvers

1. Introduction

Wary control was introduced in [1]. A full description, and results from simulations in a high-fidelity model, of the algorithm can be found there. The present paper focuses on the experimental results for the algorithm. For emergency braking, it is well known that anti-lock braking is very successful. That control algorithm does not use, nor know, the actual friction. However, the outcome, the result, depends on actual friction since the stopping distance is longer for low friction. In the same spirit, wary control is an algorithm for emergency avoidance that does not know nor use any knowledge about the value of the friction coefficient. As for braking, the result, how quickly an obstacle can be cleared, depends on actual friction. Wary control has been implemented, tested, and verified in experiments, and the results are presented in this paper.

It seems like a trivial statement that a vector has magnitude and direction. Nevertheless, this is a crucial observation for handling the fact that the actual value of friction is not known to the feedback controller. At the limit of friction a common model is an ellipse describing the maximum value of the force in terms of its components (F_x, F_y), scaled by the friction coefficient μ. If friction is not known, then the size of the friction ellipse is not known. In a critical maneuver the force will be on the friction ellipse, and the magnitude will neither be known nor possible to control. However, the direction of the total force vector on a vehicle can be swiftly controlled by individual braking of wheels, see, e.g., Chapter 6 in [2].

2. Wheel-Level Control at the Limit of Friction

At the limit of friction the possible feedback control actions at the wheel level are limited to the friction ellipse, and this is illustrated in Fig. 1. For a vehicle cornering at the limit of friction, there is a slip angle, α, that is the angle between the longitudinal x-axis of the wheel and the velocity vector of that wheel. This creates a lateral force F_{nb} where nb refers to "no braking" as shown in Fig. 1. If the wheel starts braking, a longitudinal force component will be added to the total force on the wheel. This longitudinal force will be added to F_{nb} so that there is a new resulting total force on the tire, F_b, that points at an angle θ, as is illustrated in the figure. Further, the thick line along the ellipse in Fig. 1 shows how it is possible to vary the total force, F_b, by different amounts of braking.

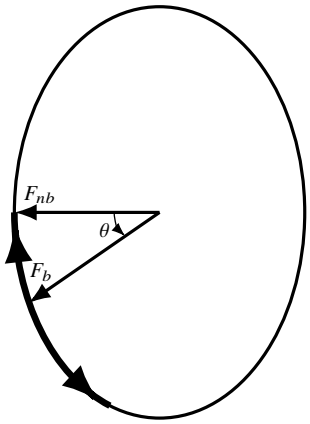

Fig. 1: Principle for wheel-level feedback control for emergency avoidance at the boundary of friction. Even though the size of the ellipse is not known, the direction of the force on the wheel can be controlled. Acting on the ellipse, at the limit of friction, means that the lateral force on the wheel when not braking, F_{nb}, can by braking be modified to a total force on the tire, F_b, at an angle θ.

In addition to pointing the force vector in a certain direction there is the possibility to brake slightly more to get a larger force component along the direction θ, see [2, Section 6.3.1]. The resulting total force vector, F_b', now pointing at an angle φ larger than θ, has the largest possible force component along the θ-direction.

2.1. Vehicle-Level Control at the Limit of Friction

The forces from each wheel add up to the total force and moment on the vehicle. Since only direction of the force vector can be controlled at the limit, this is also true for the total force on the vehicle. If the friction coefficient is known the magnitude of the total force is known, but if the friction coefficient is not known, or uncertain, we can not use the magnitude, only the direction of the total force as a basis for the feedback control algorithm.

Copyright © 2026 Society of Automotive Engineers of Japan, Inc. All rights reserved

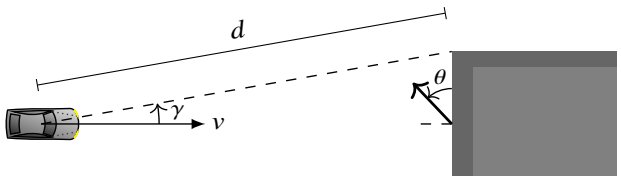

Fig. 2: An avoidance scenario, which defines the geometry parameters.

3. Emergency Avoidance

For an avoidance maneuver, the scenario is defined relating to Fig. 2. The obstacle is light gray, but rather than compensating for vehicle dimensions relative center-of-mass, it has been extended with the dark-gray area. We assume that a system for situational awareness gives the geometry parameters

- d, distance to obstacle, and
- γ, angle to avoidance point.

4. Choice of Reference Direction

In Fig. 2 the angle θ is defined related to a vertical reference. This angle is used as a reference for the direction of the force vector. When selecting the reference angle θ the two main questions are what value it should have and what the interpretation should be. Both these questions have been answered by (off-line) numerical optimization of critical vehicle maneuvers. For a friction-limited particle model, it is well known that the solution is keeping the force in a fix direction

$$\theta = \frac{\gamma + \arcsin(3\sin\gamma)}{2}, \tag{1}$$

if $\gamma \leq \arcsin(1/3)$, see [1,3](2, Section 4.3). If γ is small, (1) becomes

$$\theta \approx \frac{\gamma + 3\gamma}{2} = 2\gamma, \tag{2}$$

which means that the optimal direction of the force vector, θ, is twice the critical passing angle to the obstacle, γ. The simple expression of the relations (1) and (2) is a main reason that θ is defined in relation to the vertical axis even though γ is defined in relation to the horizontal axis.

Using a double-track model with weight transfer, wheel dynamics, and Pacejka tire models including weigthing functions, it was shown in [4] that a similar result holds for a vehicle even if it has to turn and can not change the direction of the total force vector instantaneously. The force should be optimized along the reference direction θ_v, now with v as subscript for vehicle.

5. Wary Control

Wary control is a feedback control scheme for emergency avoidance where an overview of the main ideas can be found in [2, Chapter 6] and the complete algorithm is described in [1]. The main points are:

- No knowledge of actual friction coefficient is used in the algorithm.
- High performance, which means that the performance of the feedback controller is close to that of off-line open-loop optimal control.
- Explicit algebraic expressions, which means real-time (500 or 1000 Hz).

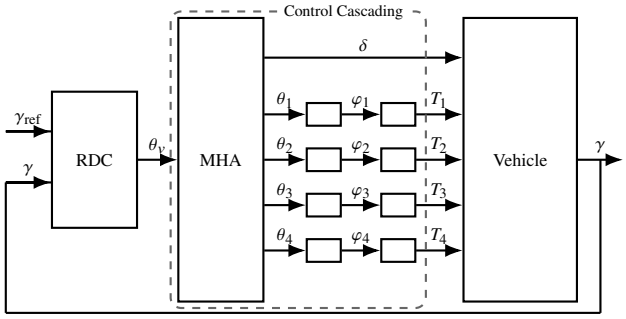

Fig. 3: The feedback control scheme for wary control. Feedback of measured and estimated vehicle states are not included in the figure.

There are a number of steps to formulate the control problem of emergency avoidance. The first step is easy. There is a vehicle with steering δ and with individual braking on each wheel T_1, T_2, T_3, T_4. This is represented by the block to the right in Fig. 3. The next step of the formulation is to define the output of the system, a reference value for it, and an output from the first controller step. Relating to Fig. 2, we want $\gamma \leq 0$, so the output is chosen as the signal γ, the angle to the avoidance point, which for a successful avoidance should decrease during the maneuver and when it reaches zero the obstacle is cleared. Since only direction of the force vector can be controlled, it is a natural first step in the controller to compute the reference angle θ_v as indicated in Fig. 3 with the box RDC (Reference Direction Computation).

The main steps in the resulting control algorithm are to use the analytical solution for the friction-limited particle model to obtain θ_v, and then to use control cascading including the modified Hamiltonian algorithm (MHA) as depicted in Fig. 3. The modified Hamiltonian algorithm is based on minimization of $F + \lambda M_z$, where F is the total force on the vehicle, M_z is the total moment, and λ is a tuning parameter to balance between the two [5]. To utilize lateral forces on the rear wheels without excessive steering variations, there is a reference model for yaw motion in combination with the MHA. The complete wary control algorithm in Fig. 3 is fully explicit, and consists of only algebraic expressions, which is the basis for real-time capability [1,2].

5.1. Control Cascading of Reference Direction

The control objective is to obtain as large as possible force component along the reference direction, θ_v (recall: not necessarily to point in that direction). This is achieved by control cascading [2, Section 6.4.1] that computes steering angle and individual wheel braking using the principles described in connection to Fig. 1, by obtaining θ_i for each wheel to compute φ_i and then T_i for each wheel. Thus, from a reference direction for the total force vector on the vehicle, the scheme is

$$\theta_v \;\rightarrow\; \theta_i \;\rightarrow\; \varphi_i \;\rightarrow\; T_i, \quad i = 1, 2, 3, 4. \tag{3}$$

Without going into details[1] about computation of δ, control cascading is illustrated in Fig. 3.

6. Principle Behavior of Wary Control

The main principle of how wary control works is illustrated in Fig. 4. The scene is a simplified version of Fig. 2 where the avoidance point is represented by the dot placed at the upper left corner of the extended obstacle in Fig. 2. The time instant when the obstacle is detected is noted with subscript 0, and then there are two more time instants illustrated that are denoted with subscripts $1, 2$.

Copyright © 2026 Society of Automotive Engineers of Japan, Inc. All rights reserved

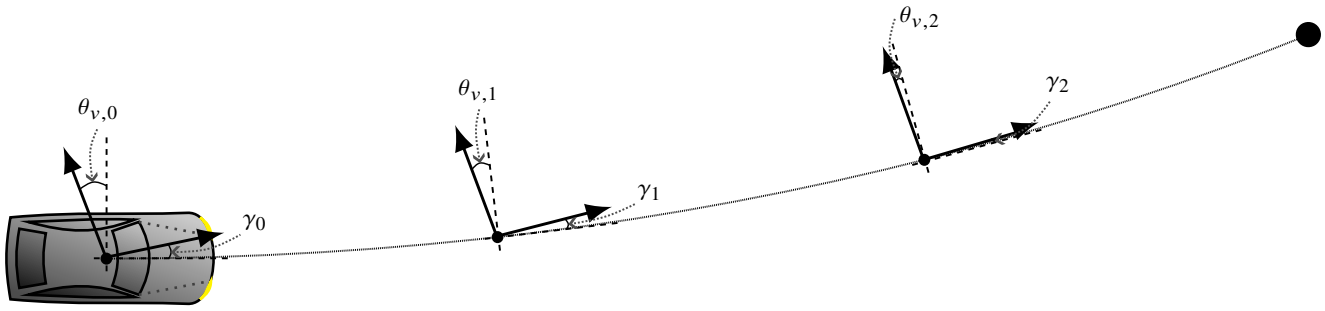

Fig. 4: An illustration of the principle function of wary control. The avoidance angle, γ, and the corresponding reference angle for the force, $\theta_v \approx 2\gamma$, successively decrease during the maneuver, and when $\gamma \leq 0$ the obstacle is cleared.

The avoidance angle γ is the angle between the path and the vector pointing at the avoidance point.

At the first time instant the avoidance angle is γ_0. The corresponding reference angle, $\theta_{v,0}$, is computed by Eq. (1). The feedback control in Fig. 3 is acting, and some time later, the position 1 is reached. At this point wary control has reduced the avoidance angle to γ_1, and the corresponding reference angle, $\theta_{v,1}$, also has decreased. At the next point, the avoidance angle γ_2, and the corresponding reference angle, $\theta_{v,2}$, has decreased even more, and as soon as $\gamma \leq 0$ the obstacle is cleared. At each point, θ_v is related to γ according to Eq. (1).

7. Experiments

Wary control has been implemented by the Dynamic Design Lab at Stanford University using the Stanford X1 vehicle as seen in Fig. 5. The vehicle is drive by wire both for steering of the front wheels and for individual wheel braking. A description of the vehicle can be found in, e.g., [6, Figure 9 and Table 1].

Fig. 5: The Stanford X1 vehicle.

7.1. Experimental Setup, $\lambda = 0$

Using X1, experiments have been performed at Thunderhill Raceway Park. The driving speed was 15 m/s (about 54 km/h or 34 mph), and the wary control algorithm takes over about 15 m before the obstacle, and it returns control to theh driver when the obstacle is cleared. With that initial speed and that short distance to the obstacle, emergency braking would not have been possible. The sampling frequency used for wary control in these experiments is 500 Hz, which is the base frequency for all logic in the vehicle via MicroAutobox II. The code for wary control could have been executed at higher frequency.

For the experiments shown in this paper, the parameter $\lambda = 0$ in the Hamiltonian $F + \lambda M_z$. This means that there is a pure focus on the force reference (recall: the *direction* of which to maximize the force vector component). This means that there is no guidance of steering to make best use of the lateral forces on the rear wheels. Nevertheless, it will be seen that wary control performs well also for this case.

8. Results

The results are shown in Figs. 6–10. As can be seen in all plots, the whole maneuver takes approximately 0.7 s, and it is doubtful if a human would be able to react within this time.

Starting with Fig. 6, the main idea for the avoidance scenario is to use an angle, θ_v, as a reference direction for the force optimization. The development of this angle during the experiment is seen in Fig. 6. As described, this angle is cascaded to each wheel, and the development for these reference angles for each wheel, θ_i, are shown in the same figure. As expected for successful clearance of the obstacle, all these angles decrease below zero at the end of the maneuver. Notice that θ_v initially increases slightly which is consistent with optimal avoidance that prioritizes initial straight braking [2, Section 4.5.1].

These reference angles are strived for by feedback control of the steering and braking, where the steering angle (desired and actual), δ, is shown in the top of Fig. 7. The same figure also shows the resulting commanded and actual slip angles, α_1, α_2, for the front wheels. These slip angles converge to desired values after slightly more than 0.1 s with some remaining wobbling for another 0.1 s.

Initially, as always for optimal avoidance (and optimal cornering), there is heavy straight braking, which is manifested in the fifth subplot of Fig. 9 showing $\psi = 0$ for the first 0.1 s of the maneuver. There is some differential braking already in this first phase of the maneuver as seen in Fig. 8 illustrating differential braking for the front axle and rear axle, respectively. Notice that braking implies that F_{x_i} is negative. Hence, the plots being positive means that there is more braking effect on the outer right wheels resulting from load transfer. Then at 0.1 s differential braking becomes more pronounceed, but successively decays as the vehicle rotates to approach its desired passing direction. In fact, as seen in both subplots, differential braking stops before the maneuver is completed, already, respectively, 0.2 s and 0.1 s before.

The reaction of the vehicle to the steering and braking is seen in Fig. 9, that shows the vehicle variables longitudinal and lateral velocity, v_x, v_y, longitudinal and lateral acceleration, a_x, a_y, yaw angle ψ, and yaw rate $\dot{\psi}$. During the maneuver, vehicle speed drops from 15 m/s to 13 m/s. As mentioned before, Fig. 9 shows vehicle behavior of straight braking for the first approximately 0.1 0.2 s. Then both $a_y, \dot{\psi}$, in the fourth and sixth subplots, are more or less constant for the remaining 0.6 s. This means that both the

Copyright © 2026 Society of Automotive Engineers of Japan, Inc. All rights reserved

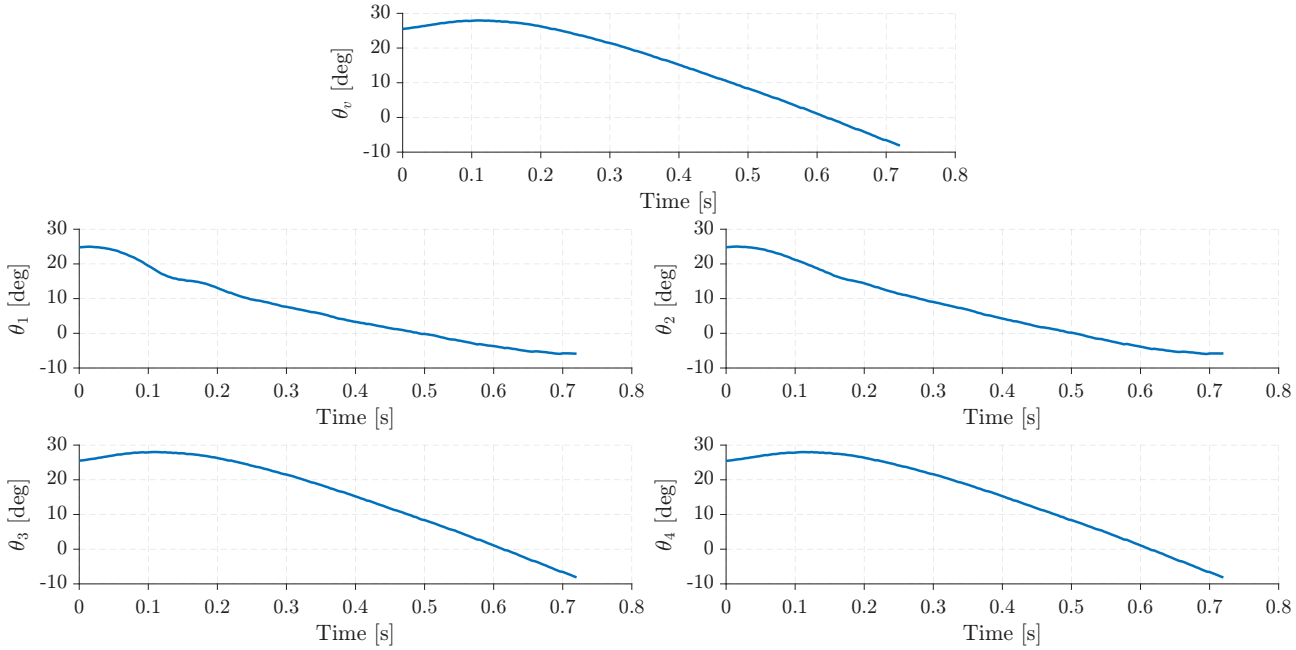

Fig. 6: Reference direction θ_v for the force acting on the vehicle, and reference directions θ_i for the force vector on each wheel obtained by control cascading.

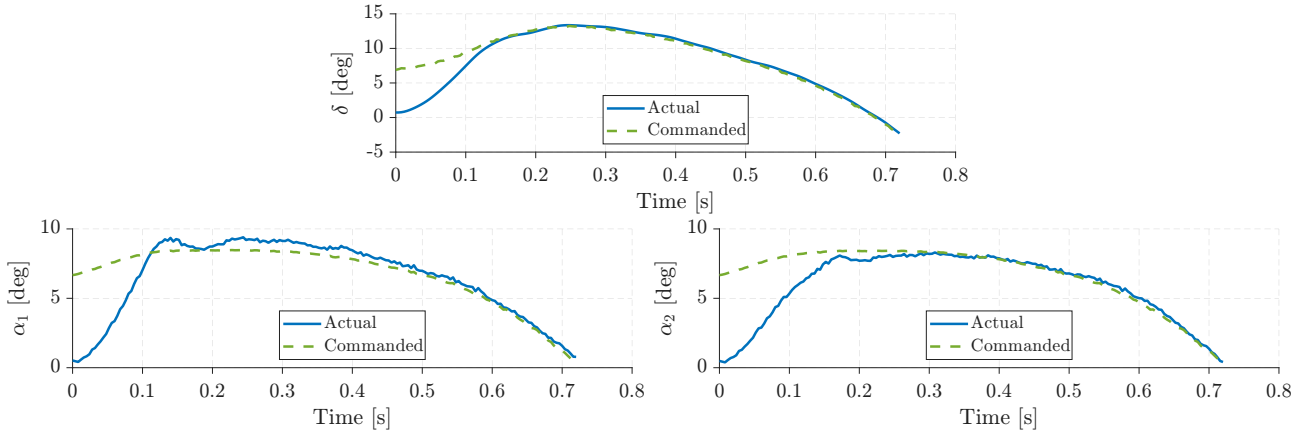

Fig. 7: Steering angle δ and slip angles on the front wheels, α_1, α_2.

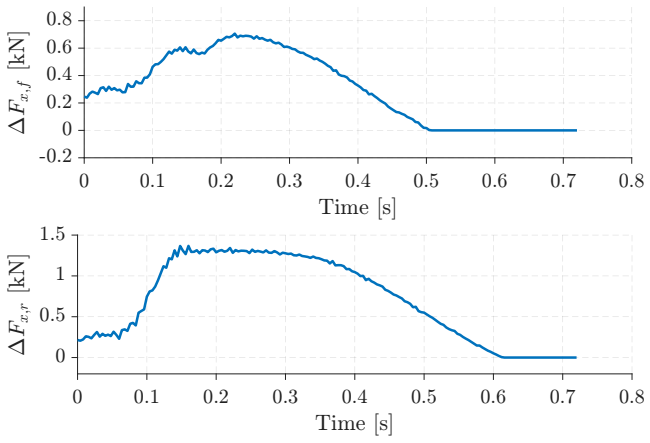

Fig. 8: Illustration of the differential braking. To the left, the difference for the front axle $\Delta F_{x,f} = F_{x_1} - F_{x_2}$ is shown, and to the right the difference for the rear axle $\Delta F_{x,r} = F_{x_3} - F_{x_4}$ is shown.

lateral velocity, v_y, in the second subplot, and the yaw angle, ψ, in the fifth subplot, for this later phase of the maneuver shows a smooth and steady growth. Overall, the vehicle behavior is stable and predictable, even though it is a really high-dynamic and fast maneuver with large lateral acceleration. Sitting in the vehicle, you are really hit in the side by the maneuver.

Finally, Fig. 10 shows the supervision variable $\mu_{\min}$, which is the lowest possible friction coefficient that would be possible to handle. As expected it goes to zero at 0.8 s, which means that the obstacle is cleared. This was also the case for θ_v in Fig. 6 and for γ, which is yet another confirmation that the obstacle is cleared.

9. Extensions

Wary control, as considered in this paper, is for one stationary obstacle, but it can be extended to a moving object, like a bicycle as in [7]. The principle of control cascading for maneuvers at the limit of friction can also be used in more complex scenarios with more than one obstacle, where some can be moving as in [8]. There,

Copyright © 2026 Society of Automotive Engineers of Japan, Inc. All rights reserved

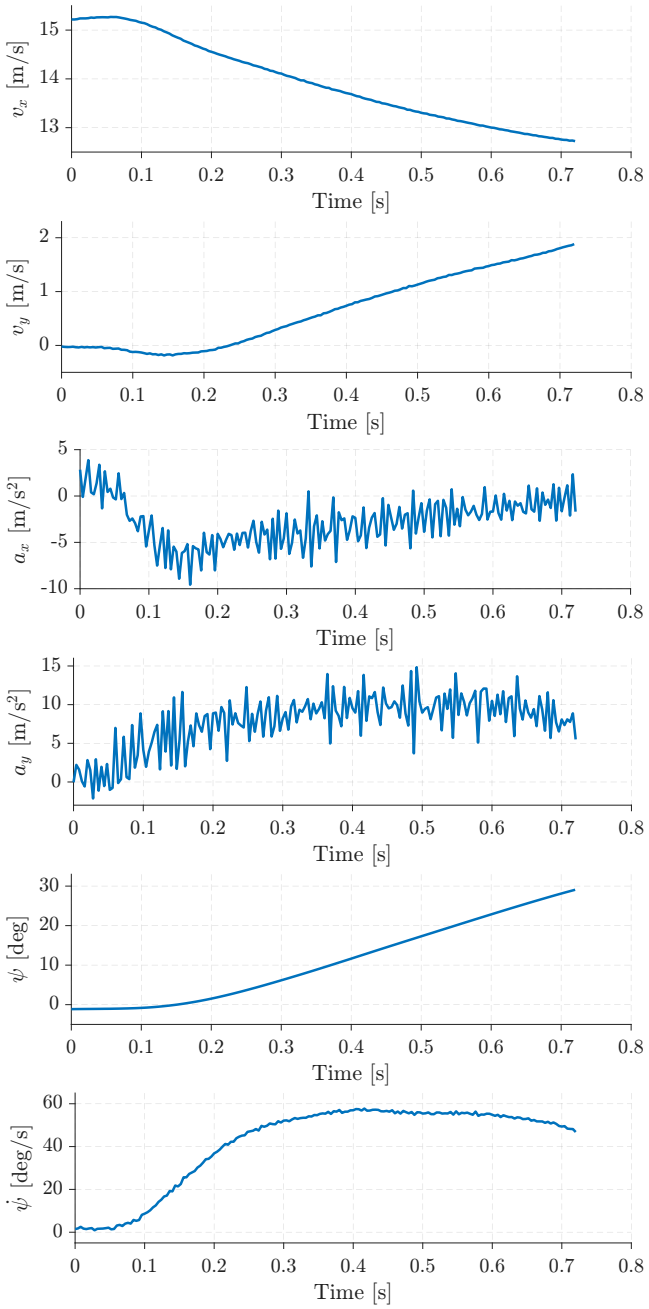

Fig. 9: Variables for the vehicle (CoG): longitudinal and lateral velocity, v_x, v_y, longitudinal and lateral acceleration, a_x, a_y, yaw angle ψ, and yaw rate $\dot{\psi}$.

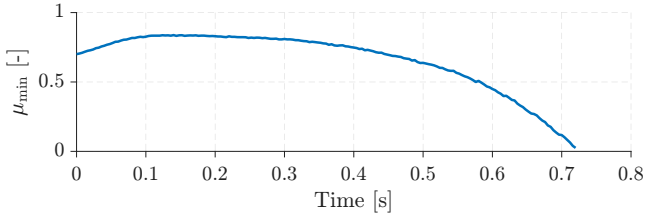

Fig. 10: The variable $\mu_{\min}$, suitable for supervision during the maneuver together with γ.

a planner is used in a slower outer loop, but control cascading is used in a fast inner loop. Thanks to the minimal computational cost, wary control can also be incorporated in other frameworks such as Multi-Modal Model Predictive Path Integral Control (MPPI)[9]. There, the wary control strategy serves as one of multiple control modes alongside maximum braking and maximum acceleration.

10. Conclusions

Already the original publication, [1], established that wary control performs well in simulation, and also exhibits almost equal performance compared to the open-loop optimal maneuver computed off-line, see, e.g., in [1, Fig. 11]. The experiments presented in this paper show that wary control works well also in real vehicle tests, and, similar to ABS, that the force component magnitude can be maximized without knowledge of its maximum magnitude. The main reasons are thanks to

- simple principles using γ and θ_v,
- realizing that vector direction can be controlled,
- and feedback control by a very efficient scheme.

11. Acknowledgments

Thank you to Elliot Weiss, Alessandra Napoli, and others in the Dynamic Design Lab for assistance with the X1 vehicle platform and experiments at the test track. The funding from the Knut and Alice Wallenberg Foundation (KAW), Sweden, from the Wallenberg AI, Autonomous Systems, and Software Program (WASP), and from the ELLIIT Strategic Area for ICT Research, supported by the Swedish Government, is gratefully acknowledged.

References

(1) Victor Fors, Björn Olofsson, and Lars Nielsen. Autonomous wary collision avoidance. *IEEE Transactions on Intelligent Vehicles*, 6(2):353–365, 2020.

(2) Lars Nielsen and Björn Olofsson. *Optimal Vehicle Maneuvers.* Publishing in 2026 by Wiley-IEEE Press, 2026. ISBN: 9781394428168, ©2026 The Institute of Electrical and Electronics Engineers, Inc.

(3) Steven C. Peters. *Optimal Planning and Control for Hazard Avoidance of Front-Wheel Steered Ground Vehicles*. Ph.D. dissertation, Department of Mechanical Engineering, Massachusetts Institute of Technology, 2012.

(4) Victor Fors, Björn Olofsson, and Lars Nielsen. Attainable force volumes of optimal autonomous at-the-limit vehicle manoeuvres. *Vehicle System Dynamics*, 58(7):1101–1122, 2020.

(5) Yangyan Gao, Mathias Lidberg, and Timothy J. Gordon. Modified Hamiltonian algorithm for optimal lane change with application to collision avoidance. *MM Science Journal*, (MAR 2015):576–584, 2015.

(6) Matthew Brown, Joseph Funke, Stephen Erlien, and J Christian Gerdes. Safe driving envelopes for path tracking in autonomous vehicles. *Control Engineering Practice*, 61:307–316, 2017.

(7) Victor Fors and J. Christian Gerdes. Wary collision avoidance of moving obstacles. *Manuscript*.

(8) Victor Fors, Pavel Anistratov, Björn Olofsson, and Lars Nielsen. Predictive force-centric emergency collision avoidance. *ASME Journal of Dynamic Systems, Measurement and Control*, 143(8):081005, 2021.

(9) Alberto Bertipaglia, Dariu M Gavrila, and Barys Shyrokau. Multi-modal model predictive path integral control for collision avoidance. *arXiv preprint arXiv:2508.21364*, 2025.

Copyright © 2026 Society of Automotive Engineers of Japan, Inc. All rights reserved